61st International Astronautical Congress, Prague, CZ.

GEOSTATIONARY STATION KEEPING CONTROL OF A SPACE ELEVATOR DURING INITIAL CABLE DEPLOYMENT

N. Takeichi
Nagoya University, Japan, takeichi@nuae.nagoya-u.ac.jp

The space elevator construction begins with the initial orbital cable deployment. However the space elevator orbit degrades due to the cable deployment, and finally the space elevator crashes to the ground without an appropriate orbital control. This paper presents an orbital control strategy to achieve the full deployment with keeping the space elevator at the geostationary position. The space elevator is modelled as a massive cable with a main spacecraft and a sinker mass on both sides, and its elasticity, flexibility and librational motion are not considered. A reference trajectory is designed so that the space elevator and its center of mass ascend vertically along the geostationary position keeping the geostationary orbital rate. From the reference trajectory equation, it is clarified that a orbital control that continuously supplies the angular momentum can lead the space elevator orbit to follow the reference one. It is also found that the reference trajectory is unstable throughout the deployment, and a linear feedback control is also derived for stabilization. Numerical simulation result clearly shows that these controls facilitates the full deployment and the geostationary station keeping of the space elevator within the feasible thrust force and total amount of fuel.

NOMENCLATURE

l	= cable length
l_o	= initial cable length, 10m
$\dot{l}$	= cable deployment rate, 1.0m/s
M	= main spacecraft mass
M_o	= initial main spacecraft mass, 19900kg
m	= sinker mass, 100kg
r	= orbital radius of main spacecraft
r_{GEO}	= GEO radius, 42164km
μ	= earth gravitational constant, 3.986×10^{14}m^3/s^2
ρ	= linear density of cable, 1.0×10^{-4}kg/m
τ	= nondimensional time, $\omega_e t$
θ	= true anomaly of main spacecraft
ω_e	= GEO rate, 7.29×10^{-5}rad/sec

I. INTRODUCTION

The space elevator construction begins with the initial orbital cable deployment[1]. After anchoring the initial cable to the ground, more cables are added by the crawling robots to enhance the elevator's strength and survivability. However, the difficulty in the initial cable deployment has been pointed out by only a few researchers[2,3]. In both papers it has been shown that the initial space elevator crashes to the ground before achieving the full deployment. To avoid such a catastrophe, some orbital control is indispensable to maintain the orbit of the initial space elevator during its deployment. Concerning the orbital control, an orbit control simulation has been carried out, and the full deployment is performed[3]. However, the detail the orbit control, such as the limitation of thrust force and the total amount of the propellant, are not discussed, and no detail of the control strategy are provided. In addition, it is estimated from the presented result that the control strategy requires quite large thrust force and propellant, and the presented control is considered to be beyond reality. It is also required for the orbital control to keep the space elevator at the geostationary position to avoid the conflict with other GEO satellites.

In this paper, it is aimed to derive a feasible orbital control strategy for the geostationary station keeping of the initial space elevator during its deployment. It is known that the center of mass of a large spacecraft no longer flies on Keplerian orbits[4,5], and it must fly higher than the GEO altitude so that their orbital periods are equal to the GEO period. Therefore, the space elevator should be controlled so that the center of mass climbs up vertically along the radial direction. This paper presents the derivation of a control strategy using the tangential thrust force, and some numerical simulations are performed.

II. EQUATIONS OF MOTION

The mathematical model of the space elevator is depicted in Fig. 1. To especially focus on the orbital motion during deployment, the elasticity and flexibility of the cable, and the fuel mass decrease due to propulsion are not considered for simplification. The cable cross-sectional area is assumed constant, and the uniform rate deployment[6] is applied. The librational motion of the cable is considered negligible because the constant rate deployment always leads the libration to be asymptotically stable[7], and its average motion is considered to hardly affect the orbital motion.

The equations of motion of the space elevator are obtained through the Lagrange formulation. The Lagrangian L of the whole system is given as follows:

$$\begin{aligned} L = &\frac{1}{2}M\left(\dot{r}^2 + r^2\dot{\theta}^2\right) + \frac{1}{2}m\left(\left(\dot{r}-\dot{l}\right)^2 + \left(r-l\right)^2\dot{\theta}^2\right) \\ &+\frac{1}{2}\rho l\left(\left(\dot{r}-\dot{l}\right)^2 + \left(r^2 - rl + \frac{l^2}{3}\right)\dot{\theta}^2\right) \\ &-\mu\left(-\frac{M}{r} - \frac{m}{r-l} - \rho\ln\frac{r}{r-l}\right) \end{aligned} \quad (1)$$

Through the Lagrange formulation the following equations of motion are obtained:

$$\begin{aligned} &M\ddot{r} + \left(m+\rho l\right)\left(\ddot{r}-\ddot{l}\right) + \dot{M}\dot{r} + \rho\dot{l}\left(\dot{r}-\dot{l}\right) = \\ &\quad -\mu\left(\frac{M}{r^2} + \frac{m}{\left(r-l\right)^2} + \frac{\rho l}{r^2 - rl}\right) \\ &\quad +\left(Mr + m\left(r-l\right) + \rho l\left(r - \frac{1}{2}l\right)\right)\dot{\theta}^2 \end{aligned} \quad (2)$$

$$\begin{aligned} &\left(Mr^2 + m\left(r-l\right)^2 + \rho l\left(r^2 - rl + \frac{l^2}{3}\right)\right)\ddot{\theta} = \\ &\quad -\dot{\theta}\left(2Mr\dot{r} + 2m\left(r-l\right)\left(\dot{r}-\dot{l}\right) + \rho\dot{l}\left(r^2 - rl + \frac{l^2}{3}\right)\right. \\ &\quad \left.+\dot{M}r^2 + \rho l\left(2r\dot{r} - \dot{r}l - r\dot{l} + \frac{2}{3}l\dot{l}\right)\right) + Q_\theta \end{aligned} \quad (3)$$

, where Q_θ is a generalized force corresponding to the tangential thrust force. The mass of the main spacecraft and the cable length are given as follows:

$$M = M_o - \rho l, \quad \dot{M} = -\rho\dot{l} \quad (4)$$

$$l = l_o + \dot{l}t, \quad \ddot{l} = 0 \quad (5)$$

After normalizing the variables by r_{GEO} and ω_e, the following set of the equations of motion is obtained:

$$\begin{aligned} &M\hat{r}'' + \left(m+\hat{\rho}\hat{l}\right)\left(\hat{r}''-\hat{l}''\right) + \hat{M}'\hat{r}' + \hat{\rho}\hat{l}'\left(\hat{r}'-\hat{l}'\right) = \\ &\quad -\left(\frac{M}{\hat{r}^2} + \frac{m}{\left(\hat{r}-\hat{l}\right)^2} + \frac{\hat{\rho}\hat{l}}{\hat{r}^2 - \hat{r}\hat{l}}\right) \\ &\quad +\left(M\hat{r} + m\left(\hat{r}-\hat{l}\right) + \hat{\rho}\hat{l}\left(\hat{r} - \frac{1}{2}\hat{l}\right)\right)\theta'^2 \end{aligned} \quad (6)$$

$$\begin{aligned} &\left(M\hat{r}^2 + m\left(\hat{r}-\hat{l}\right)^2 + \hat{\rho}\hat{l}\left(\hat{r}^2 - \hat{r}\hat{l} + \frac{\hat{l}^2}{3}\right)\right)\hat{\theta}'' = \\ &\quad -\hat{\theta}'\left(2M\hat{r}\hat{r}' + 2m\left(\hat{r}-\hat{l}\right)\left(\hat{r}'-\hat{l}'\right) + \hat{\rho}\hat{l}'\left(\hat{r}^2 - \hat{r}\hat{l} + \frac{\hat{l}^2}{3}\right)\right. \\ &\quad \left.+\hat{M}'\hat{r}^2 + \hat{\rho}\hat{l}\left(2\hat{r}\hat{r}' - \hat{r}'\hat{l} - \hat{r}\hat{l}' + \frac{2}{3}\hat{l}\hat{l}'\right)\right) + \hat{Q}_\theta \end{aligned} \quad (7)$$

, where $\mu = \omega_e^2 r_{GEO}^3$, prime (') denotes the differentiation by the nondimensional time $\tau = \omega_e t$, and the normalized variables are denoted by ^. The normalized equations are analyzed hereafter.

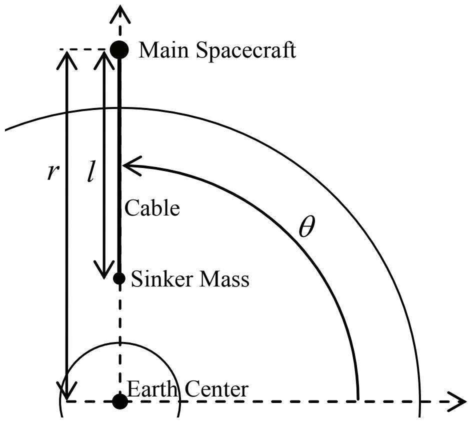

Fig. 1 Space Elevator Model

III. UNCONTROLLED BEHAVIOR

As presented in the previous studies, the space elevator crashes to the ground without any orbital control. The uncontrolled behaviour is obtained by a numerical simulation giving the situation where the center of mass flies on the GEO radius as the initial condition. The orbital radius time-histories of the main spacecraft, sinker mass, and the center of mass are shown in Fig. 2. In the beginning 10days of the deployment, the center of mass stays almost at the GEO altitude, the main spacecraft ascends, and the sinker mass descends as expected by the previous studies[1]. However, the main spacecraft turns to descent around 80th day, and finally the whole system crashes to the ground. Without an orbital control, the angular momentum of the whole system is conservative. However the orbital angular momentum of the space elevator decreases as the cable deployment because the body angular momentum increases. In this way, the whole system begins descent toward the ground. In this case, the space elevator orbits faster than the geostationary rate as shown in Fig. 3 in the same way as common satellites.

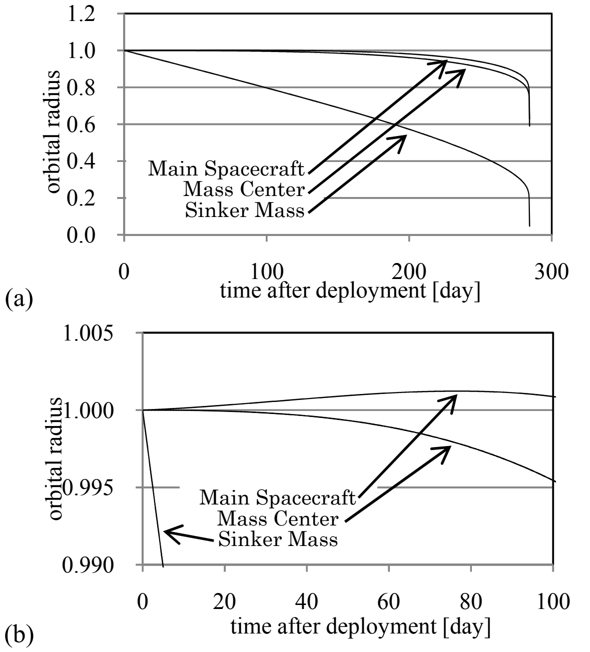

Fig. 2 Uncontrolled Behavior: Orbital Radius, a: Whole History, b: Beginning Stage Detail

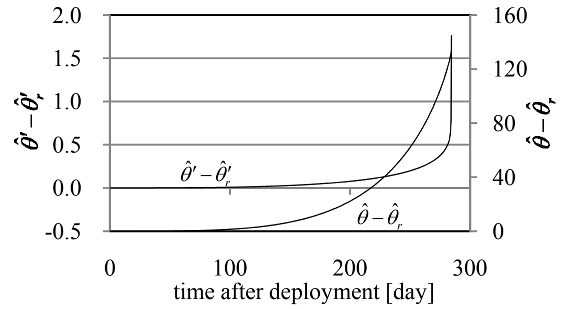

Fig. 3 Uncontrolled Behavior: $\hat\theta' - \hat\theta_r'$ and $\hat\theta - \hat\theta_r$

IV. CONTROL STRATEGY

Reference Trajectory

As mentioned above, the space elevator should be controlled to keep the geostationary position to avoid conflict with other GEO satellites. Therefore the orbital control should lead the main spacecraft to ascent vertically. To derive the control strategy, a reference trajectory is assumed. By substituting $\hat r = \hat r_r + \delta\hat r$ and $\hat\theta = \hat\theta_r + \delta\hat\theta$, where $\hat r_r$ and $\hat\theta_r$ are the reference ones, the following equations are obtained through linearization:

$$\left(M+m+\hat\rho\hat l\right)\hat r_r'' - \hat\rho\hat l'^2 = -\left(\frac{M}{\hat r_r^2}+\frac{m}{\left(\hat r_r-\hat l\right)^2}+\frac{\hat\rho\hat l}{\hat r_r^2-\hat r_r\hat l}\right) + \left(M\hat r_r + m\left(\hat r_r-\hat l\right)+\hat\rho\hat l\left(\hat r_r-\frac{1}{2}\hat l\right)\right) \tag{8}$$

$$\left(2M\hat r_r\hat r_r' + 2m\left(\hat r_r-\hat l\right)\left(\hat r_r'-\hat l'\right)+\hat\rho\hat l'\left(-\hat r_r\hat l+\frac{\hat l^2}{3}\right) + \hat\rho\hat l\left(2\hat r_r\hat r_r' - \hat r_r'\hat l - \hat r_r\hat l' + \frac{2}{3}\hat l\hat l'\right)\right) = \hat Q_{\theta r} \tag{9}$$

$$\left(M+m+\hat\rho\hat l\right)\delta\hat r'' = +\left(2\left(M+m+\hat\rho\hat l\right)\hat r_r - 2m\hat l - \rho\hat l^2\right)\delta\hat\theta' - \left(\left(\frac{2M}{\hat r_r^3}+\frac{2m}{\left(\hat r_r-\hat l\right)^3}+\frac{\hat\rho\hat l\left(\hat l-2\hat r_r\right)}{\hat r_r^2\left(\hat r_r-\hat l\right)^2}\right) + \left(M+m+\hat\rho\hat l\right)\right)\delta\hat r \tag{10}$$

$$\left(M\hat r_r^2 + m\left(\hat r_r-\hat l\right)^2 + \hat\rho\hat l\left(\hat r_r^2-\hat r_r\hat l+\frac{\hat l^2}{3}\right)\right)\delta\hat\theta'' = -\left(2M\hat r_r\hat r_r' + \left(2m\left(\hat r_r-\hat l\right)+\hat\rho\hat l\left(\hat l-2\hat r\right)\right)\left(\hat r_r'-\hat l'\right)\right)\delta\hat\theta' - 2\left(\left(M+m+\hat\rho\hat l\right)\hat r_r' - \left(m+\hat\rho\hat l\right)\hat l'\right)\delta\hat r - \left(2M\hat r_r + 2m\left(\hat r_r-\hat l\right)+\hat\rho\hat l\left(2\hat r_r-\hat l\right)\right)\delta\hat r' + \delta\hat Q_\theta \tag{11}$$

, where $\hat\theta_r = \tau$, $\hat\theta_r' = 1$=geostationary rate, $\hat\theta_r'' = 0$, and $\hat Q_\theta = \hat Q_{\theta r} + \delta\hat Q_\theta$.

Angular Momentum Supplying Control

Eq. (9) is equivalent to the following equation:

$$\frac{d}{d\tau}\left(M\hat r_r^2 + m\left(\hat r_r-\hat l\right)^2 + \hat\rho\hat l\left(\hat r_r^2-\hat r_r\hat l+\frac{\hat l^2}{3}\right)\right) = \hat Q_{\theta r} \tag{12}$$

The left hand of this equation is the time differentiation of the total angular momentum of the reference trajectory. Therefore, it is expected that the orbital control, that supplies the orbital angular momentum so that the space elevator has the same angular momentum as that the one on the reference trajectory has, will pull up the main spacecraft along the geostationary position.

The reference radius of the main spacecraft $\hat{r}_r$ is designed so that the space elevator flies on a circular orbit with the geostationary rate at every moment, and is numerically obtained by letting the left hand of Eq. (8) be equal to zero. The reference trajectory is shown in Fig. 4. The numerical result applying the orbital control given in Eq. (12) is shown in Fig. 5. Although the orbital radius of the main spacecraft follows the reference one in the beginning stage of the deployment as shown in Fig. 5a, the deviation gradually increases as shown in Fig. 5b and c, and abruptly diverges around the 400th day. This result implies the instability of the orbital motion during deployment. To investigate the stability the linearized equations (10) and (11) are rewritten in the following form:

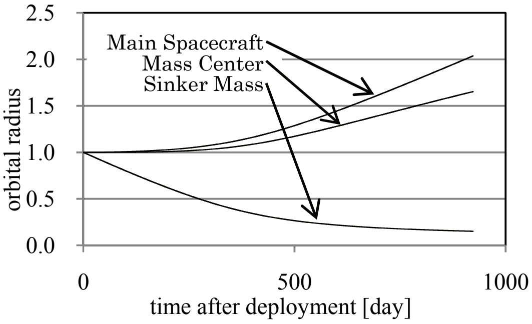

Fig. 4 Reference Trajectory: Orbital Radius

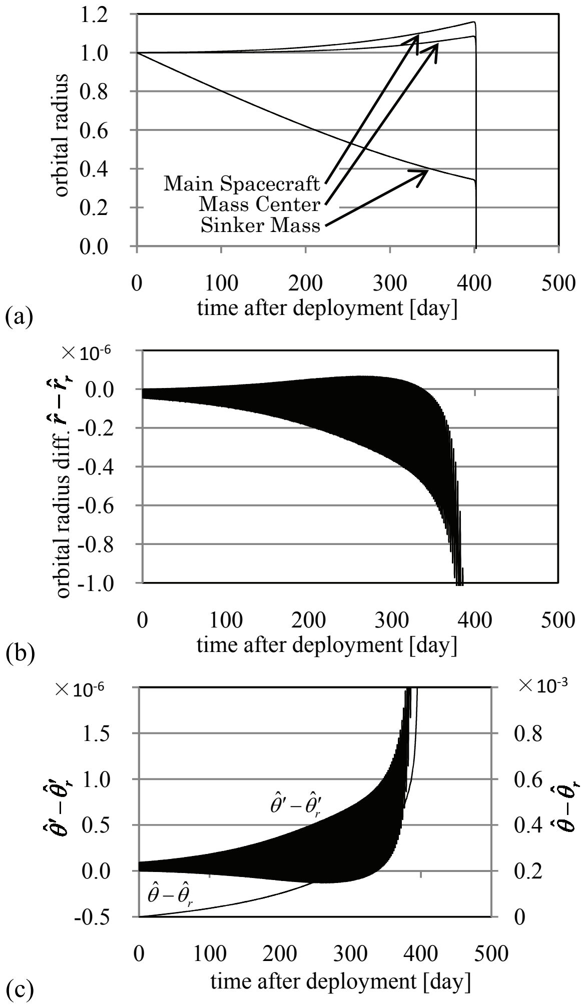

Fig. 5 Controlled Behavior with $Q_{\theta r}$, a: orbital radius, b: $\hat{r}-\hat{r}_r$, c: $\hat{\theta}'-\hat{\theta}'_r$ and $\hat{\theta}-\hat{\theta}_r$

$$\delta\hat{\mathbf{x}}' = \mathbf{A}\delta\hat{\mathbf{x}} + \mathbf{B}\mathbf{u} = \mathbf{A}\delta\hat{\mathbf{x}} + \mathbf{B}\frac{\delta\hat{Q}_\theta}{I_T} \tag{13}$$

, where $\delta\mathbf{x}$, $\mathbf{A}$, $\mathbf{B}$, M_T, and I_T are defined as follows:

$$\delta\hat{\mathbf{x}} = \begin{pmatrix}\delta\hat{r} & \delta\hat{r}' & \delta\hat{\theta} & \delta\hat{\theta}'\end{pmatrix}^T \tag{14}$$

$$\mathbf{A} = \begin{pmatrix} 0 & 1 & 0 & 0 \\ A_{21} & 0 & 0 & A_{24} \\ 0 & 0 & 0 & 1 \\ A_{41} & A_{42} & 0 & A_{44} \end{pmatrix} \tag{15}$$

$$A_{21} = -\frac{1}{M_T}\left(\frac{2M}{\hat{r}_r^3} + \frac{2m}{\left(\hat{r}_r-\hat{l}\right)^3} + \frac{\hat{\rho}\hat{l}\left(\hat{l}-2\hat{r}_r\right)}{\hat{r}_r^2\left(\hat{r}_r-\hat{l}\right)^2}\right) - 1 \tag{16}$$

$$A_{24} = \left(2\hat{r}_r - \frac{2m\hat{l}+\hat{\rho}\hat{l}^2}{M_T}\right) \tag{17}$$

$$A_{41} = \frac{-2\left(\left(M+m+\hat{\rho}\hat{l}\right)\hat{r}_r' - \left(m+\hat{\rho}\hat{l}\right)\hat{l}'\right)}{I_T} \tag{18}$$

$$A_{42} = \frac{-\left(2M\hat{r}_r + 2m\left(\hat{r}_r-\hat{l}\right) + \hat{\rho}\hat{l}\left(2\hat{r}_r-\hat{l}\right)\right)}{I_T} \tag{19}$$

$$A_{44} = \frac{-\left(2M\hat{r}_r\hat{r}_r' + \left(2m\left(\hat{r}_r-\hat{l}\right) + \hat{\rho}\hat{l}\left(\hat{l}-2\hat{r}\right)\right)\left(\hat{r}_r'-\hat{l}'\right)\right)}{I_T} \tag{20}$$

$$\mathbf{B} = \begin{pmatrix}0 & 0 & 0 & 1\end{pmatrix}^T \tag{21}$$

$$M_T = M + m + \hat{\rho}\hat{l} \tag{22}$$

$$I_T = \left(M\hat{r}_r^2 + m\left(\hat{r}_r-\hat{l}\right)^2 + \hat{\rho}\hat{l}\left(\hat{r}_r^2 - \hat{r}_r\hat{l} + \frac{\hat{l}^2}{3}\right)\right) \tag{23}$$

M_T is the total mass of the space elevator, and I_T can be regarded as its orbital moment of inertia. To clarify the stability of the orbital motion, the eigenvalues with $\hat{Q}_{\theta r}$ and $\delta\hat{Q}_\theta = 0$ are numerically obtained, and the maximum value of their real part is shown in Fig. 6. It is found that the orbital motion is unstable throughout the deployment as shown in Fig. 6a and b, and especially strongly unstable beyond about 400th day as shown in

Fig. 6a. This eigenvalue analysis result agrees with the numerical simulation result. Hence some feedback control is necessary to stabilize the orbital motion around the reference trajectory.

Linear Feedback Control

Although the system described in Eq.(13) is inherently a time varying system, all the components are monotonous functions. Therefore, it is expected that even a simple linear feedback control can stabilize the reference trajectory. A linear feedback control is derived through the linear quadratic regulator using the parameters at the end of deployment, where the orbital motion posses the strongest instability. The cost function and the parameters used in the LQR are as follows:

$$J = \int_0^\infty \left(\delta \mathbf{x}^T \mathbf{Q} \delta \mathbf{x} + \mathbf{u}^T \mathbf{R} \mathbf{u} \right) d\tau \tag{24}$$

$$\mathbf{A} = \begin{pmatrix} 0 & 1 & 0 & 0 \\ 13.2 & 0 & 0 & 3.30 \\ 0 & 0 & 0 & 1 \\ -1.14\times10^{-4} & -1.08 & 0 & -2.38\times10^{-4} \end{pmatrix} \tag{25}$$

$$\mathbf{Q} = \mathbf{I}\,,\ R = 1 \tag{26}$$

The feedback control is derived as follows:

$$\delta \hat{Q}_\theta = I_T \left(-41.9\delta\hat{r} - 10.6\delta\hat{r}' + \delta\hat{\theta} - 8.29\delta\hat{\theta}' \right) \tag{27}$$

The maximum value of the real part of the eigenvalues of the orbital motion with $\delta \hat{Q}_\theta$ given in Eq. (27) is shown in Fig. 7. It is suggested that it is possible to stabilize the linearized orbital motion through this

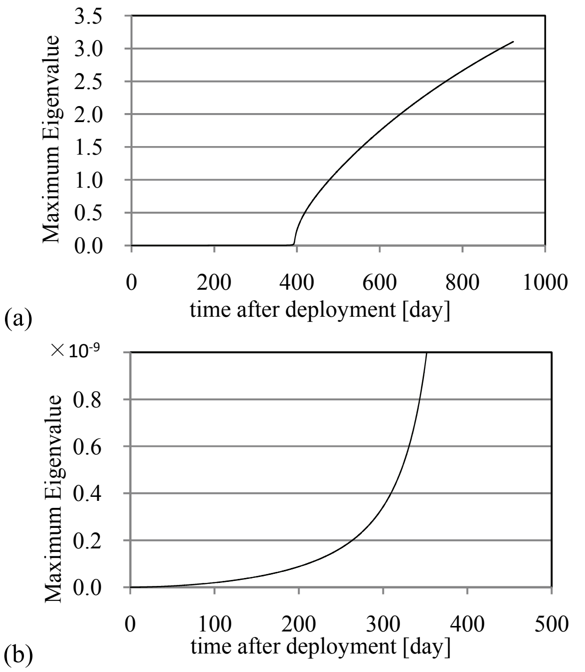

Fig. 6 Max Real Part of Eigenvalues of Linearized Orbital Motion with $Q_{\theta r}$, a: whole history, b: beginning half detail

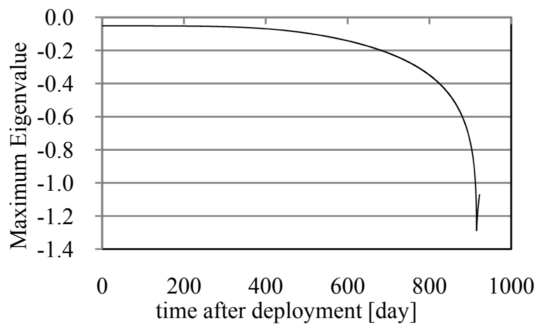

Fig. 7 Max Real Part of Eigenvalues of Linearized Orbital Motion with Feedback Control δQ_θ

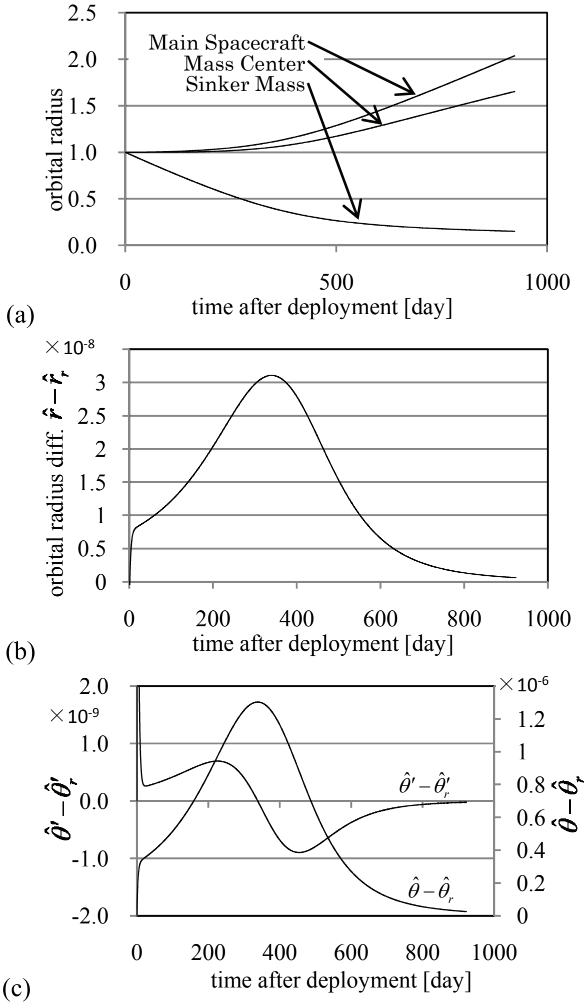

Fig. 8 Controlled Behavior with Feedback Control, a: orbital radius, b: $\hat{r}-\hat{r}_r$, c: $\hat{\theta}'-\hat{\theta}'_r$ and $\hat{\theta}-\hat{\theta}_r$

feedback control. The numerical simulation results are shown in Fig. 8. This result clearly shows that the orbital motion has been stabilized to follow the reference trajectory, and the space elevator deployment has been successfully performed with keeping the geostationary position.

According to the principal of virtual work as follows:

$$\delta W = Q_\theta \cdot \delta\theta = \mathbf{F_T} \cdot \mathbf{v}\delta t = F_T \cdot r\delta\theta \quad (28)$$

, the thrust force of a thruster equipped on the main spacecraft F_T is given as follows:

$$F_T = \frac{Q_\theta}{r} \quad (29)$$

The time history of the thrust force is shown in Fig. 9. It is clear that the thrust force below 2N is required for the full deployment of the space elevator. The maximum thrust force is only 1.73N, and the required fuel mass for orbital control is 2121.5kg in total assuming I_{SP} =4000sec. These values can be recognized to be in the practical ranges.

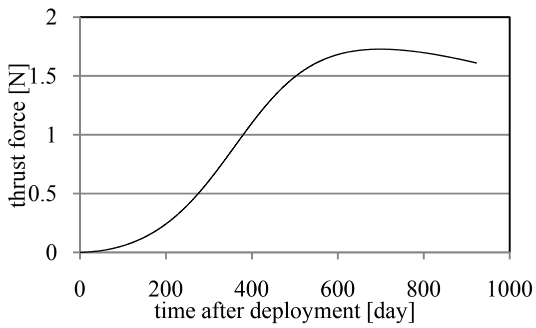

Fig. 9 Orbital Control Thrust Force

V. CONCLUSION

The fundamental orbital control to achieve the full-length deployment and the geostationary station keeping of an initial space elevator is presented. The reference trajectory is designed so that the space elevator fly on a circular orbit with the geostationary rate. It is found that an orbital control that supplies the angular momentum can lead the space elevator to follow the reference trajectory. In addition a linear feedback control is introduced to stabilize the reference trajectory. Numerical simulation result has shown that both the maximum thrust force and required fuel mass are in feasible ranges.

In this study, the most simplified model has been analyzed. Therefore more detailed analyses using sophisticated models including librational motion, flexibility, elasticity, and diameter taper of the cable, mass decrease due to propulsion, etc. must be carried out in the future works. It is also important to clarify the cause of instability and its abrupt change during deployment. Further optimization of the control strategy is also possible. Because the linearized system is a linear parameter varying system as mentioned above, a gain schedule control should be applied. It will also be possible to find a more practical control strategy such as the one that flattens the thrust force by controlling the deployment rate, etc.

REFERECNES

1 Edwards, B.C., “Design and Development of a Space Elevator,” Acta Astronautica, Vol. 47, No. 10, pp. 735-744, 2000.

2 Mantri, P., “Deployment Dynamics of Space Tether Systems,” Doctoral Degree Dissertation, Graduate Faculty of North Carolina State University, Raleigh, North Carolina, 2007.

3 Lang, D.D., “Space Elevator Initial Construction Mission Overview,” available online: http://home.comcast.net/~GTOSS/

4 Beletskii, V. V., “Motion of an Artificial Satellite about Its Center of Mass,” NASA TT F-429, 1966.

5 Takeichi, N., Natori, M. C., Okuizumi, N., and Higuchi, K., “Periodic Solutions and Controls of Tethered Systems in Elliptic Orbits,” Journal of Vibration and Control, Vol. 10, No. 10, Oct. 2004, pp. 1393-1413.

6 von Flotow, A. H., and Laue, J. H., “Deployment of a Tethered Satellite Pair into Low Earth Orbit for Plasma Diagnostics,” Journal of the Astronautical Sciences, Vol. 34, No. 1, 1986, pp. 65–90.

7 Takeichi, N., Natori, M.C., and Okuizumi, N., “Fundamental Strategies for Control of a Tethered System in Elliptical Orbits,” Journal of Spacecraft and Rockets, Vol. 40, No. 1, Jan.–Feb. 2003, pp. 119-125.